Journal of Nuclear Medicine, published on January 5, 2023 as doi:10.2967/jnumed.122.264656

Detection of early esophageal neoplastic Barrett lesions with quantified fluorescence molecular endoscopy using cetuximab-800CW

Short running title: Detecting esophageal neoplasia with FME

Ruben Y. Gabriëls[1], MD; Lisanne E. van Heijst[1*], Wouter T.R. Hooghiemstra[1], Anne M. van der Waaij[1], MD; Gursah Kats-Ugurlu[2], MD, PhD; Arend Karrenbeld[2], MD; Dominic J. Robinson[3], PhD; Anna Tenditnaya[4,5]; Vasilis Ntziachristos[4,5], PhD; Dimitris Gorpas[4,5], PhD; Wouter B. Nagengast[1], MD, PhD*

1 Department of Gastroenterology and Hepatology, University of Groningen, University Medical Center Groningen, Groningen, The Netherlands

2 Department of Pathology and Medical Biology, University of Groningen, University Medical Center Groningen, Groningen, The Netherlands

3 Center for Optic Diagnostics and Therapy, Otolaryngology, Erasmus University Medical Center, Rotterdam, The Netherlands

4 Technical University of Munich, Germany, School of Medicine, Central Institute for Translational Cancer Research (TranslaTUM), Chair of Biological Imaging

5 Helmholtz Zentrum München (GmbH), Neuherberg, Germany, Institute of Biological and Medical Imaging

**Authors contributed equally*

Word count: 4858

Number of figures: 6

Number of tables: 2

Corresponding Author: Wouter B. Nagengast

Phone: +31(50) 361 61 61

Fax: +31(50) 361 93 31

E-mail: w.b.nagengast@umcg.nl

Postal address: Department of Gastroenterology and Hepatology, University Medical Center Groningen, Hanzeplein 1, PO Box 30.001, 9700 RB, Groningen, The Netherlands

ABSTRACT

Esophageal adenocarcinoma (EAC) causes 6 % of cancer-related deaths worldwide. Near-infrared fluorescence molecular endoscopy (NIR-FME) uses a tracer that targets overexpressed proteins. In this study we aim to investigate the feasibility of an epidermal growth factor receptor (EGFR) targeted tracer, cetuximab-800CW, to improve detection of early-stage EAC. **Methods:** We validated EGFR expression in 73 esophageal tissue sections. Subsequently, we topically administered cetuximab-800CW and performed high-definition white-light endoscopy (HD-WLE), narrow band imaging (NBI) and NIR-FME in fifteen patients with Barrett's esophagus (BE). Intrinsic fluorescence values were quantified using multi-diameter single fiber reflectance (MDSFR) and single-fiber fluorescence (SFF) spectroscopy. Back-table imaging, histopathological examination and EGFR immunohistochemistry on biopsies collected during NIR-FME procedures were performed and compared to *in vivo* imaging results. **Results:** Immunohistochemical pre-analysis showed high EGFR expression in 67% of dysplastic tissue sections. NIR-FME visualized all 12 HD-WLE visible lesions and 5 HD-WLE invisible dysplastic lesions, with increased fluorescence signal in visible dysplastic BE lesions compared to non-dysplastic BE as shown by MDSFR/SFF, reflecting a target-to-background ratio (TBR) of 1.5. Invisible dysplastic lesions also showed increased fluorescence with a TBR of 1.67. Immunohistochemistry analysis showed EGFR overexpression in 16 out of 17 (94%) dysplastic BE lesions, which all showed fluorescence signal. **Conclusion:** This study has shown that NIR-FME using cetuximab-800CW can improve detection of dysplastic lesions missed by HD-WLE and NBI.

INTRODUCTION

Esophageal cancer is responsible for approximately 6% of cancer related deaths worldwide, with studies predicting a rise in the incidence of esophageal adenocarcinoma (EAC) (1). Late stage detection leads to a five-year survival rate of 15 – 20% (2).

Surveillance of Barrett's esophagus (BE) is performed by high-definition white-light endoscopy (HD-WLE) and narrow band imaging (NBI) combined with random biopsies following the Seattle protocol to detect early EAC lesions (3). A study performing a follow-up endoscopy procedure one year after the primary endoscopy detected 24% more EAC lesions (4). This indicates a high miss-rate by HD-WLE and NBI in combination with random biopsies during endoscopic surveillance (4,5).

In the quest for improving the detection of early-stage EAC, near-infrared fluorescence molecular endoscopy (NIR-FME) has recently shown potential to improve performance over the current endoscopic standard (6). A phase I trial conducted here at the University Medical Center Groningen (UMCG) employed the tracer bevacizumab-800CW, targeting vascular endothelial growth factor A (VEGF-A), and showed ~33% improvement of early lesion detection compared to conventional HD-WLE and NBI (7).

NIR-FME can provide additional guidance in histopathological assessment and has shown to reduce sampling error (8,9). This technique in combination with the tracer cetuximab-800CW, targeting epidermal growth factor receptor (EGFR), has been described to provide additional real-time information assisting intraoperative decision-making aiding tumor delineation (10). Recently, multiplexed imaging was successfully introduced where two fluorescently labelled tracers targeting EGFR and human epidermal growth factor receptor 2 (HER2) were evaluated for the detection of EAC (11).

In the quest for improving the detection of early-stage EAC, we validated EGFR expression in Barrett lesions and aimed to investigate the feasibility of NIR-FME with cetuximab-800CW, an EGFR targeted tracer, to improve detection of early-stage EAC in Barrett patients compared to HD-WLE and NBI.

MATERIALS AND METHODS

This phase I feasibility study with cetuximab-800CW is embedded in an ongoing intervention study performed at the UMCG (NCT03877601). All included patients are priorly diagnosed with low-grade dysplasia (LGD), high-grade dysplasia (HGD), or early-stage EAC at a regional hospital and referred to the UMCG, which is the BE expert center for the northern Netherlands. Included patients underwent HD-WLE combined with a NIR-FME procedure using the topical administration of cetuximab-800CW (12).

Inclusion and Exclusion Criteria

For the immunohistochemistry pre-analysis we have included esophageal endoscopic mucosal resection (EMR) specimens of 25 patients. Following all pre-analysis study procedures, we selected and included fifteen patients eligible for cetuximab-800CW administration. These patients were priorly diagnosed with LGD, HGD or early-stage EAC and scheduled for an endoscopic procedure. Patients received both oral and written information regarding study procedures and the tracer cetuximab-800CW. Patients < 18 years old, allergic to immunoglobulins, pregnant or breastfeeding were excluded. Additionally, patients who received prior cetuximab treatment, radiation therapy, chemotherapy, immunotherapy, or surgery for esophageal cancer were excluded. All patients interested in participating in either the *ex vivo* pre-analysis or the *in vivo* procedure with administration of cetuximab-800CW prior to endoscopy had to give informed consent within two weeks but not earlier than 48 hours after receiving information. The study design of the current study is shown in figure 1.

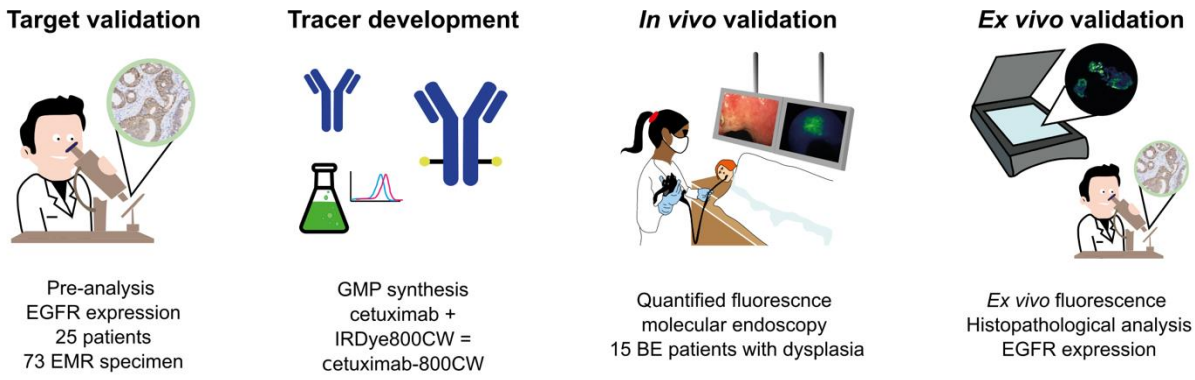

FIGURE 1: Overview of the study design.

Ex Vivo Pre-analysis EGFR Expression

Ex vivo pre-analysis was performed by two independent researchers, RYG and LEvH, to investigate EGFR expression. EMR specimens were formalin fixed for 24 hours and specimens were histologically sliced into 4 µm tissue slices (n = 73), which were then stained for hematoxylin and eosin, P53 and EGFR. The slices were scanned by Hamamatsu NanoZoomer (Hamamatsu Photonics, Japan) and viewed with NDP.view2. H-scores were independently and blindly calculated by RYG and LEvH to quantify the EGFR staining intensity.

Synthesis of Cetuximab-800CW

Production of cetuximab-800CW (peak excitation/emission at 778/795 nm) was performed in the cleanroom facility of the Clinical Pharmacy and Pharmacology department of the UMCG (12).

Fluorescence Molecular Endoscopy combined with Spectroscopy

Real-time *in vivo* NIR-FME with cetuximab-800CW was achieved by coupling a fiberscope (Schölly Fiberoptic GmbH, Denzlingen, Germany) to the SurgVision Explorer Endoscope (SVEE, SurgVision BV., Groningen, The Netherlands), which is based on a system previously developed by our group (13).

Multi-diameter single fiber reflectance (MDSFR) and single-fiber fluorescence (SFF) spectroscopy, developed by the University Medical Center Rotterdam, Erasmus MC, was employed as a reference for the NIR-FME measurements (14,15). The process leading to the quantification of tracer's intrinsic fluorescence was previously described (14,15). Both NIR-FME and MDSFR/SFF were performed through the working channel of standard endoscope.

Procedure

HD-WLE and NBI were performed for general evaluation of the Barrett segment and suspected lesions. Acetyl cysteine 0.1 % was used for mucus reduction during the procedure. Following a five-minute incubation of the topically administered cetuximab-800CW, the esophagus was rinsed with water to remove abundant, unbound tracer. We administered 1 ml of 0.1 mg/ml cetuximab-800CW per 1 cm of Barrett segment. NIR-FME was performed to examine the esophagus and investigate whether all HD-WLE suspected lesions could be detected and whether additional lesions, missed by HD-WLE/NBI, could be identified. We calculated the target-to-background ratio (TBR), the ratio between the mean NIR-FME image pixel intensities from the region of interest (ROI, e.g., lesion of fluorescence foci) and the non-dysplastic Barrett's esophagus (NDBE), determined as the background. The mean value of each ROI was calculated for those pixels within the upper 70% of the corresponding histogram.

To assess the quality of the data acquired with the FME system, we calculated the signal-to-background noise ratio (SNR) in dB scale and contrast-to-noise ratio (CNR) for every frame containing visible or invisible lesions (16). The reliability of the data was then assessed through the Rose criterion for CNR and the 95% confidence level of a measurement for the SNR, which requires CNR > 3 and SNR > 6 dB for a lesion to be distinguishable from the background (17).

Subsequently, HD-WLE guided, spectroscopy was performed to measure the intrinsic fluorescence of cetuximab-800CW from the NIR-FME identified suspected and/or invisible lesions. All measurements were done in triplicate and the mean values were used for the quantification of the cetuximab-800CW fluorescence, serving as control measurements for the validation of NIR-FME findings (18).

Ex Vivo Analysis

Tissue biopsies were collected from non-suspected Barrett tissue, lesions, and invisible lesions during *in vivo* NIR-FME procedures. They were then formalin fixed and paraffin embedded (FFPE). From these specimens, 10 μm tissue sections were deparaffinized and imaged with the Odyssey CLx flatbed scanner (LI-COR Biosciences, Lincoln, Nebraska, USA), while 4 μm thick sections were stained with hematoxylin and eosin and P53 and subsequently histopathologically analyzed by the pathologists GK-U and AK. Immunohistochemistry on EGFR staining was performed on additional 4 μm tissue sections, after which they were scanned by Hamamatsu NanoZoomer (Hamamatsu Photonics, Japan) and digitally analyzed using NDP.view2. H-scores were calculated to quantify the staining intensity of EGFR by the two researchers RYG and LEvH. A total of 32 formalin fixed tissue sections stained with EGFR were analyzed.

Statistical Analysis

Analyses and graph layout were implemented using GraphPad Prism (version 8.4.2, GraphPad Software Inc, San Diego, California, USA). Normality tests were performed on all data. Descriptive statistics were performed to calculate mean and standard deviation of the H-scores and Pearson correlation was used to assess the interobserver agreement of manual H-scoring by the two independent researchers. H-scores, TBRs, *in* and *ex vivo* spectroscopy data were analyzed by one-way ANOVA (ANalysis Of VAriance). P values < 0.05 were considered statistically significant. All data are displayed as mean ± standard deviation.

Ethical Considerations

Approval of this study was obtained from the Medical Ethics Committee at the UMCG (METc Number 2018/701).

RESULTS

Ex Vivo EGFR Expression Analysis

In total 73 FFPE tissue slices were analyzed for EGFR expression levels and histopathology. Pathologists AK and GK-U selected areas containing NDBE, LGD, HGD, and EAC. H-score quantification showed that most of the dysplastic BE (DBE) tissue (LGD, HGD and EAC) scored intermediate and high membranous staining (n = 49, 67%) (figure 2). However, 24 DBE tissue areas were negatively/low scored (33%). Subsequently, the H-score for EGFR of NDBE tissue was negative/low in 33 tissue areas (89%). The calculated mean H-score for NDBE was 57 ± 38 and significantly lower than LGD 127 ± 58 ($P < 0.0001$), HGD 130 ± 60 ($P < 0.0001$) and EAC 126 ± 73 ($P < 0.0001$). The fraction of variance between the two researchers was calculated with the Pearson correlation coefficient r = 0.9056 (figure 2).

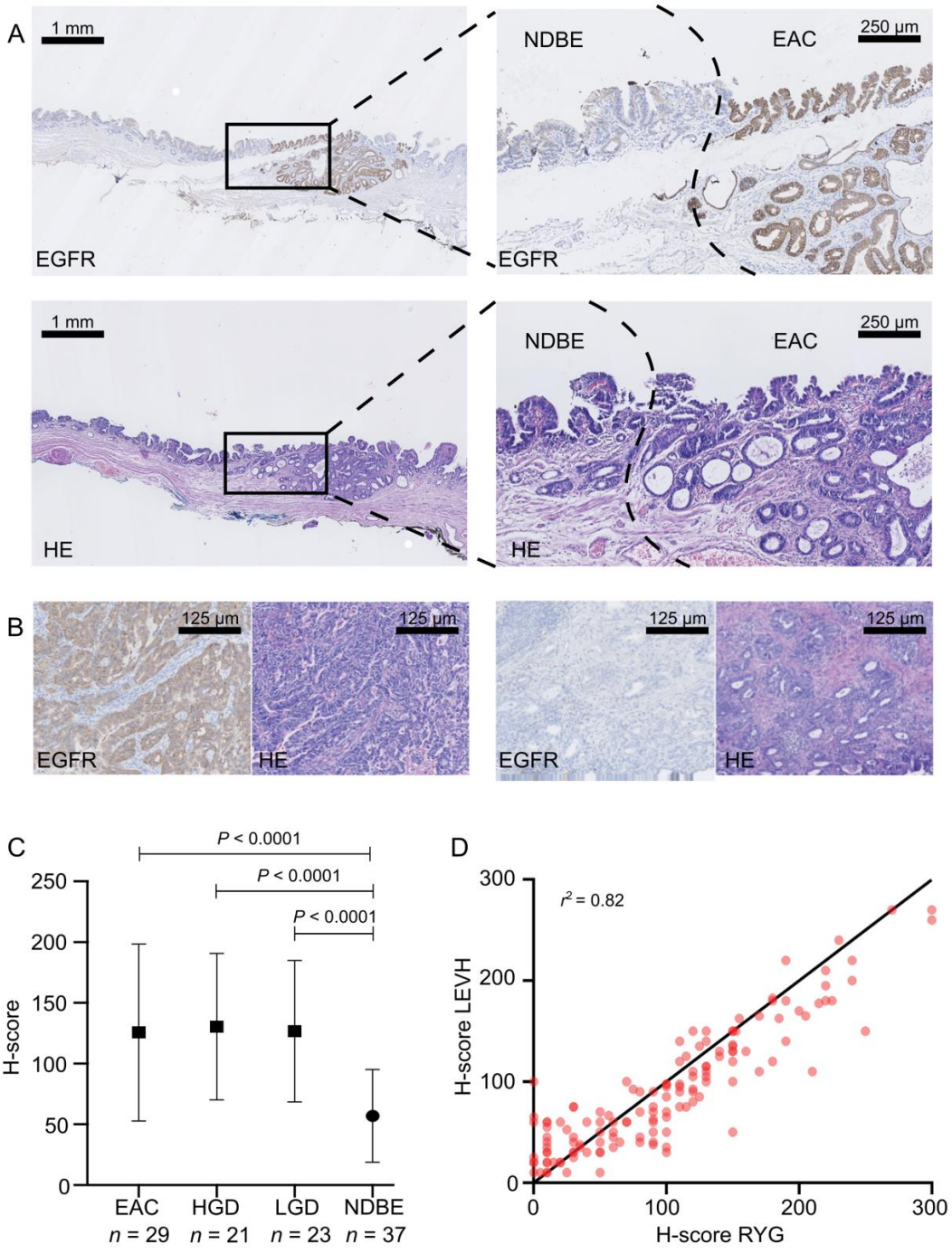

FIGURE 2: A: Immunohistochemistry results of EGFR staining, brown staining (top) and hematoxylin and eosin staining, purple staining (bottom) with the left images at low magnification (5x) and the right images at high magnification (20x) with pathological delineation of EAC and NDBE. B: Histopathological tissue slices at high magnification (40x) display high staining of EAC on the left and no staining of EAC on the right, showing variable EGFR expression. C: H-scoring was performed by two independent researchers of which the means and standard

deviation are displayed for EAC, HGD, LGD and NDBE. D: Scoring consistency between two independent researchers was determined with the Pearson correlation coefficient.

Patient Characteristics

Fifteen patients, two females and thirteen males were included in the trial. All included patients received cetuximab-800CW during the procedure and none of the patients experienced any (serious) adverse events. An overview of patient characteristics is displayed in table 1.

Near-infrared Fluorescence Molecular Endoscopy

All 9 lesions detected by the referring endoscopist at the regional hospitals were detected by our BE expert endoscopist WBN. Furthermore, our BE expert endoscopist additionally detected 3 flat lesions by HD-WLE that were not described by the referring endoscopist. All 12 HD-WLE visible lesions were visualized by the NIR-FME camera showing increased fluorescence intensity. Histopathological assessment conducted by a BE expert pathologist showed dysplasia in all visible and invisible lesions. We observed clear *ex vivo* fluorescence signal on the epithelial side of all biopsies in dysplastic lesions.

The TBRs of the complete delineated visible lesions resulted in a mean of 1.3 ± 0.2 ($P < 0.0001$), while the invisible lesions presented a higher mean TBR of 1.6 ± 0.2 ($P < 0.0001$). We could not detect a lesion using either HD-WLE or the NIR-FME system in one patient referred with LGD and additional random biopsies according to the Seattle protocol did not detect dysplasia either. Distribution of mean TBR values per tissue and per patient are shown in figure 3. Data quality assessment showed an average SNR of 21.79 ± 1.65 dB and an average CNR of 4.54 ± 1.57, both being above the corresponding critical values for discrimination between lesion and background, as defined in table 2.

In five patients, NIR-FME detected areas which did not show morphological changes suspicious for dysplasia by HD-WLE or NBI. These areas showed dysplasia on histology and thus counted as invisible lesions by standard imaging technology (figure 4).

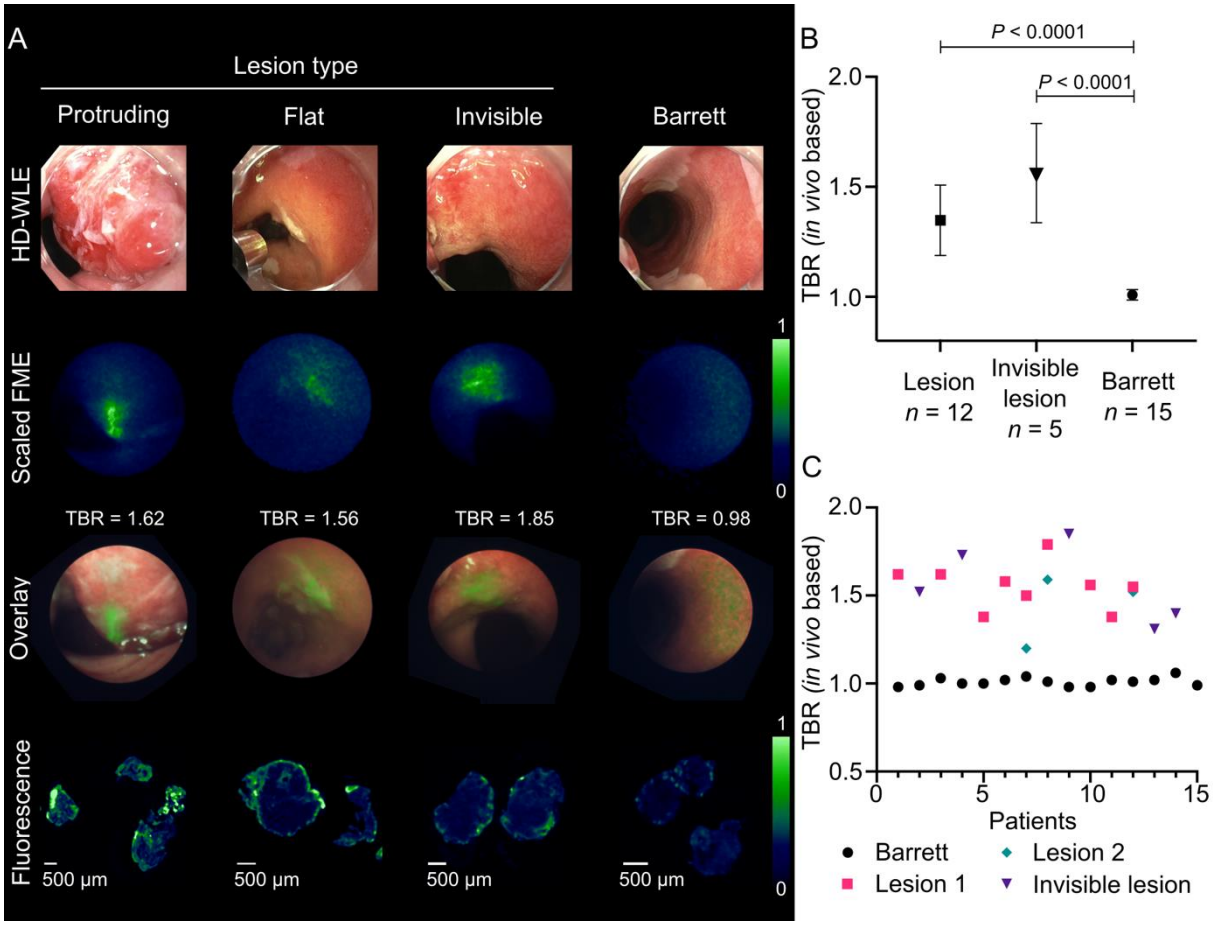

FIGURE 3: A. Different lesion and tissue types visualized with different imaging techniques. From top to bottom are shown the HD-WLE images, the corresponding frames acquired with the NIR-FME system in fluorescence channel, the overlay of color and fluorescence data acquired with NIR-FME and ex vivo fluorescence images acquired with the Odyssey CLx flatbed scanner. The fluorescence images were linearly normalized to the common global maximum (1) and minimum (0) values to enable visual comparison of the signal strength between the different lesion types. Graphs B and C show the calculated TBRs combined and in every single patient separately, respectively.

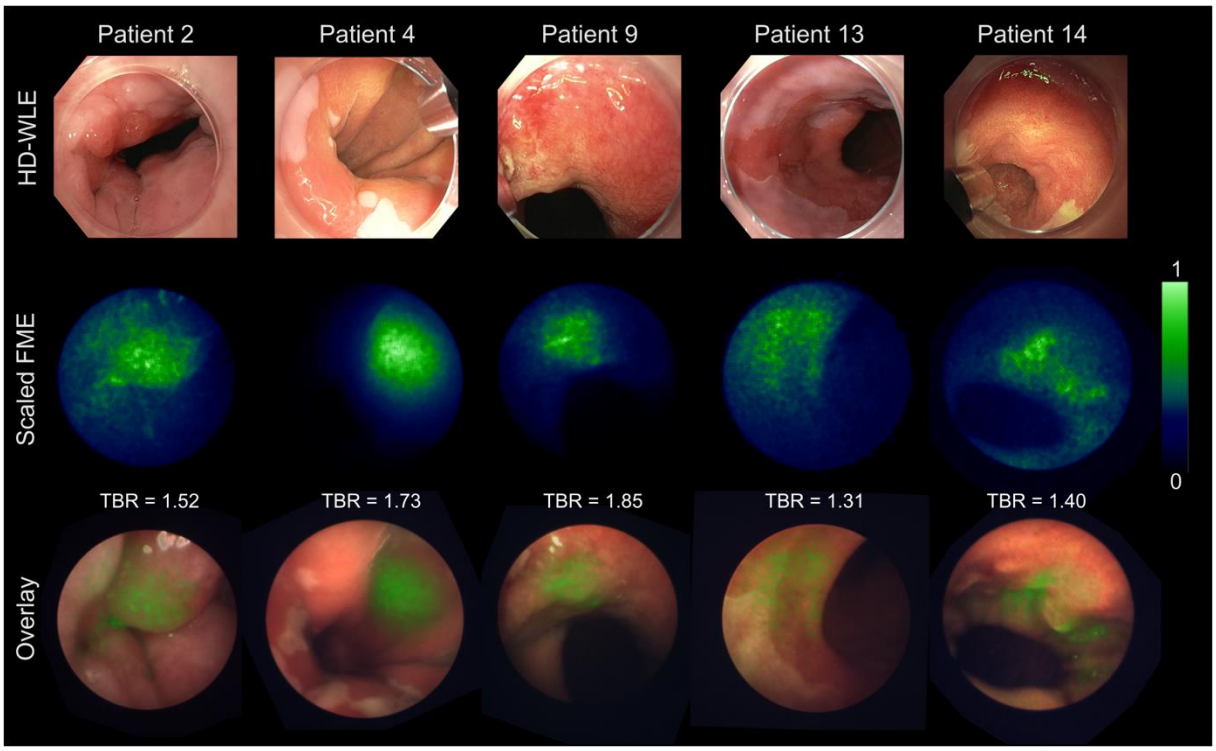

FIGURE 4: HD-WLE invisible dysplastic lesions detected by NIR-FME. From top to bottom are shown the HD-WLE images, the corresponding NIR-FME fluorescence images of the HD-WLE invisible lesions and the overlay of the NIR-FME color and fluorescence data from five different patients. All fluorescence images were normalized in regards to their individual maximum (1) and minimum (0) values to enable visual assessment of the fluorescence localization.

In Vivo MDSFR/SFF Spectroscopy

MDSFR/SFF spectroscopy measurements were performed to quantify intrinsic fluorescence values of the tracer *in vivo* by correcting for optical properties of the tissue. Measurements of NDBE were completed in all patients, with a mean tracer's intrinsic fluorescence of 0.012 ± 0.003 $Q \cdot \mu^{f}_{a,x}$. The mean value for visible lesions (n = 10) was calculated from 30 measurements which resulted in a higher mean of 0.018 ± 0.004 $Q \cdot \mu^{f}_{a,x}$ when compared to NDBE (P = 0.0014), with a spectroscopy TBR of 1.5. These findings are comparable to the *in vivo* analysis of the raw fluorescence images. *In vivo* spectroscopy measurements were not feasible in two

lesions. In one of the lesions, it was impossible to perform reliable measurements because of the angle of spectroscopy fiber towards the lesion. In the other lesion, the spectroscopy measurements failed because we had unstable contact between the lesion and the fiber. Invisible lesions (n = 5) showed a higher mean of 0.020 ± 0.005 $Q \cdot \mu^{f}_{a,x}$ when compared to NDBE (P = 0.0003). This results in a calculated spectroscopy TBR of 1.67, confirming the data from the *in vivo* raw fluorescence image analysis of HD-WLE invisible lesions. *In vivo* spectroscopy results are shown in figure 5.

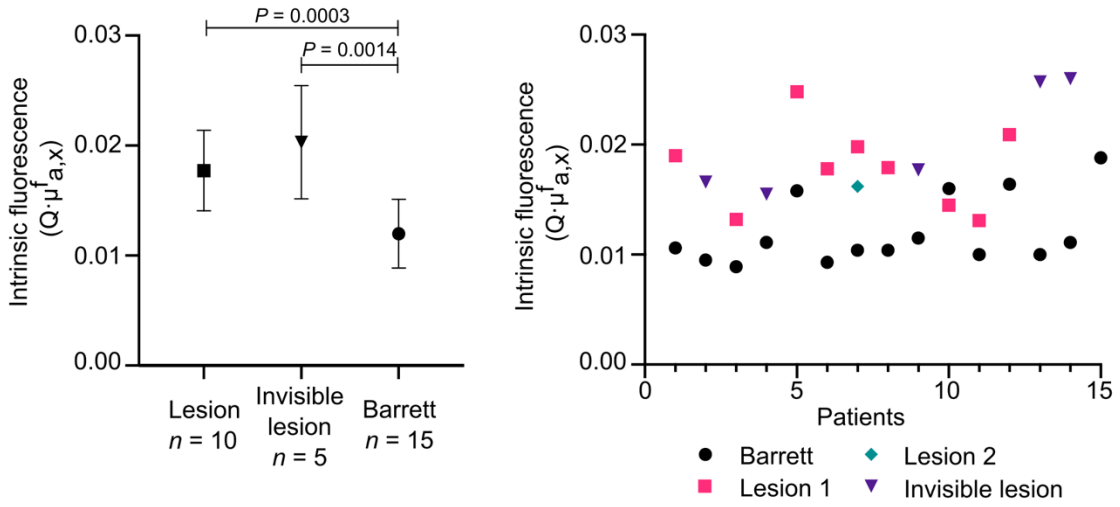

FIGURE 5: In vivo spectroscopy results. On the left, in vivo spectroscopy differences between HD-WLE visible lesions, HD-WLE invisible lesions and NDBE are shown. On the right, in vivo spectroscopy fluorescence values for NDBE, HD-WLE visible lesions and HD-WLE invisible lesions within each patient are shown.

Ex Vivo EGFR Expression

All 17 dysplastic esophageal lesions showed moderate to strong *ex vivo* fluorescence signal. LGD was found in 2 tissue slices, HGD in 6 tissue slices and EAC in 9 tissue slices. NDBE was found in 15 tissue slices collected from endoscopically non-suspected Barrett tissue. Examples of EGFR expression levels in the samples are shown in figure 6. H-score quantification showed that 94% of DBE tissue (LGD, HGD and EAC) collected from visible and invisible

lesions scored intermediate or high epithelial EGFR staining. NDBE tissue showed *ex vivo* negative fluorescence signal and lower EGFR expression H-score results compared to HGD and EAC tissue.

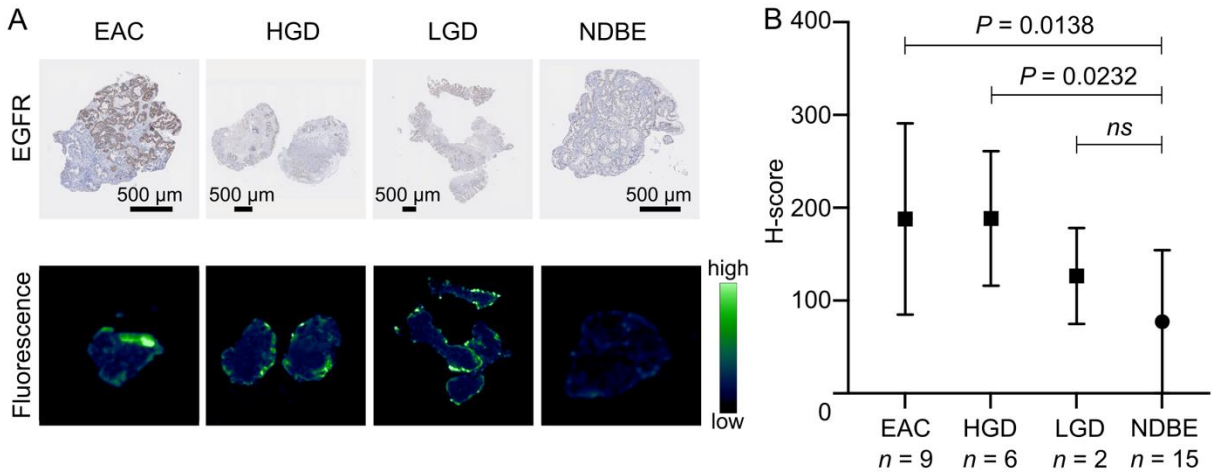

FIGURE 6: EGFR expression and ex vivo fluorescence in different tissue types. The top row shows tissue slices with EGFR staining. The bottom row shows corresponding deparaffinized tissue slices scanned with the Odyssey CLx flatbed scanner showing fluorescence at the luminal side of the tissue where the tracer was sprayed. The graph displays the calculated H-score of EGFR staining.

DISCUSSION

Early detection of DBE and early-stage EAC can prevent the progression towards locally advanced EAC and thereby improve morbidity and mortality rates significantly. In the current study, we investigated EGFR expression in DBE and early-stage EAC tissue. Furthermore, we tested the safety and feasibility of cetuximab-800CW *in vivo* to improve (pre)malignant esophageal lesion detection with NIR-FME in BE. Our immunohistochemistry pre-analysis showed intermediate to high EGFR expression within 67% of the dysplastic areas. NIR-FME with cetuximab-800CW detected all visible dysplastic lesions and additionally revealed 5 dysplastic lesions missed using HD-WLE/NBI. The specificity of the results was confirmed by two independent BE expert pathologists and 16 out of the 17 dysplastic lesions (94%) showed intermediate or high EGFR expression levels. This signifies the ability of cetuximab-800CW to visualize dysplastic areas in BE, even if morphological abnormalities cannot be detected by HD-WLE/NBI.

Results from our previous *in vivo* feasibility study with the tracer bevacizumab-800CW showed that NIR-FME could improve early lesion detection significantly (7). Another published phase I proof-of-concept study demonstrated the feasibility of using an EGFR targeted tracer in combination with a tracer targeting HER2 for the detection of early EAC lesions by using dual spectral endoscopic imaging (11). However, EGFR or HER2 expression analysis was not performed and *in vivo* imaging results were not quantified (11). The follow-up clinical trial, showed an *in vivo* TBR of 1.5 using an EGFR targeted tracer in 31 patients, although additional lesions were not detected (19). In our phase I clinical trial, we found that the EGFR targeted tracer, cetuximab-800CW, detected all known dysplastic lesions and, more importantly, detected 5 invisible dysplastic lesions confirmed by histopathology, which also showed to be EGFR positive. Quantified NIR-FME improves early lesion detection by 29% compared to the current

clinical standard using HD-WLE/NBI endoscopy. We quantified EGFR expression in an extensive pre-analysis in esophageal EMR specimens and subsequently in all esophageal biopsies taken during the NIR-FME procedure. Moreover, we confirmed our *in vivo* NIR-FME findings with unbiased spectroscopy measurements.

Our *ex vivo* analysis regarding the biopsies showed a relatively high EGFR expression within dysplastic esophageal tissue. One reason for these high EGFR expression levels compared to literature might be our relatively small patient sample size from the phase 1 trial in which we analyzed EGFR expression. All 17 NIR-FME identified lesions, HD-WLE visible and invisible lesions, showed *in vivo* fluorescence after incubation with cetuximab-800CW, suggesting that when lesions are EGFR positive, they can be detected by cetuximab-800CW. However, one lesion did not show clear EGFR expression in the *ex vivo* analysis which might be caused by sampling error during biopsy.

Fluorescence molecular imaging can be further developed and improved by addressing several study limitations. We solely included referred BE patients with a suspected lesion. Consequently, our cohort mainly consists of patients with EAC, resulting in a distorted representation of the overall BE population. Research has shown that endoscopists at regional, non-BE expert centers, detect significantly fewer EAC lesions compared to endoscopists at a BE expert center (20). This means that we most likely detected more suspected lesions using HD-WLE compared to referring centers, which could indicate that this novel red flag imaging technique is of even greater value for regional, non-BE expert, centers. It would be of great interest to include non-BE experts in a follow-up study to evaluate the level of impact of this technique. We manually calculated the TBRs from *in vivo* images by comparing the fluorescence signal of the region for the area of interest to the unspecific fluorescence signal of a region for NDBE. A reason for these relatively low TBRs could be the heterogenous distribution of the

topically administrated tracer. Another limitation is that we were not able to visualize the tracer on a microscopic level. The obtained biopsies were directly formalin fixed after the endoscopic procedure. Our previous study with bevacizumab-800CW demonstrated that the tracer is almost entirely washed away during the paraffin embedding resulting in a loss of fluorescence signal (13). However, in the best possible manner, *ex vivo* images made with the Odyssey fluorescence flatbed scanner, showed a clear signal only in the luminal side of the tissue. Finally, we were not able to take real time spectroscopy measurements. All measurements were calculated and analyzed after completion of all the study procedures. Since we needed the endoscopic working channel for both fluorescence molecular endoscope and spectroscopy fibers, we could not measure the intrinsic fluorescence and search for the most intense fluorescent spot simultaneously. This could explain why we did not measure a higher fluorescence signal in the lesion compared to the background in one of the included patients.

The last few years, several new imaging techniques have been developed to improve early EAC lesion detection in Barrett patients. Amongst them are computer aided diagnosis (CAD) algorithms (21), which could be used as a second assessor. CAD already performs better at EAC detection than general endoscopists with HD-WLE images alone, showing a sensitivity of 93% versus 72% and a specificity of 83% versus 74% (22). We envision that HD-WLE and FME assisted by CAD can further improve detection rates of early EAC lesions with the aim to make the Seattle protocol redundant and improve patient outcome.

In conclusion, we validated that EGFR is overexpressed in (pre)malignant esophageal tissue, the latter does not impede the use of an EGFR targeted tracer in combination with NIR-FME. We demonstrated *in vivo* that this novel red flag imaging technique in combination with cetuximab-800CW, has potential to improve early lesion detection in Barrett patients. We expect

that a dual spectral imaging study using an EGFR targeted tracer in combination with a VEGF-A targeted tracer can further improve detection of early (pre)malignant lesions in these patients.

ACKNOWLEDGEMENTS

The authors acknowledge support by the European Union's Horizon 2020 TRANSCAN-2 funding mechanism (project TRANSCAN-147, ESCEND) and the Dutch Cancer Society, Amsterdam, the Netherlands and Horizon 2020 project SENSITIVE (Grant agreement ID: 801347).

CONTRIBUTIONS

Guarantor of the article: Wouter B. Nagengast

Specific author contributions: All authors were involved in conceptualization and study design. WBN, DG and VN were responsible for funding acquisition and resources. Pathologists GK-U and AK blindly analyzed the hematoxylin and eosin coupes for dysplasia. RYG and LEvH independently performed H-scoring data analysis and visualization. RYG, LEvH, WTRH, AMW and WBN performed all *in vivo* study procedures. RYG and LEvH performed all *ex vivo* procedures subsequently. DJR performed the spectroscopy analysis. AT and DG contributed to the interpretation and designed software to analyze the imaging results. RYG and LEvH wrote the first draft of the manuscript. WTRH, AM, AT, DG, VN and WBN contributed to results interpretation and critically reviewed the manuscript.

All authors approved the final version of the manuscript, including the authorship list.

STATEMENT OF DISCLOSURE

The authors have declared that no competing interests exists.

KEYWORDS

Barrett's esophagus, cetuximab, epidermal growth factor receptor, esophageal adenocarcinoma, fluorescence molecular imaging

ABBREVIATIONS

BE: Barrett's esophagus, DBE: dysplastic Barrett's esophagus; CAD: computer aided diagnosis; CNR: contrast-to-noise ratio; EAC: esophageal adenocarcinoma; EGFR: epidermal growth factor receptor; EMR: endoscopic mucosal resection; FFPE: formalin-fixed and paraffin-embedded; FME: fluorescence molecular endoscopy; HER2: human epidermal growth factor receptor 2; HGD: high-grade dysplasia; LGD: low-grade dysplasia; MDSFR: multi-diameter single-fiber reflectance; NBI: narrow-band imaging; NDBE: non-dysplastic Barrett's esophagus; NIR: near-infrared; ROI: region-of-interest; SNR: signal-to-background noise ratio; SFF: single-fiber fluorescence; TBR: target-to-background ratio; UMCG: University Medical Center Groningen; VEGF-A: Vascular endothelial growth factor A.

KEY POINTS

Does NIR-FME in combination with cetuximab-800CW, an EGFR targeted tracer, improve detection of early-stage EAC.

This study adds an extensive *ex vivo* pre-analysis of EGFR expression in esophageal dysplastic and non-dysplastic tissue. *In vivo,* we additionally detected 5 HD-WLE invisible lesions and we further quantified *in vivo* fluorescence results with spectroscopy and validated these results *ex vivo* with EGFR expression levels.

Dual spectral NIR-FME including an EGFR targeted tracer will further improve detection of (pre)malignant lesions in the esophagus.

REFERENCES

1. Sung H, Ferlay J, Siegel RL, et al. Global Cancer Statistics 2020: GLOBOCAN estimates of incidence and mortality worldwide for 36 cancers in 185 countries. *CA Cancer J Clin*. 2021;71:209-249.
2. Alsop BR, Sharma P. Esophageal cancer. *Gastroenterol Clin North Am*. 2016;45:399-412.
3. Sharma P, Hawes RH, Bansal A, et al. Standard endoscopy with random biopsies versus narrow band imaging targeted biopsies in Barrett's oesophagus: a prospective, international, randomised controlled trial. *Gut*. 2013;62:15-21.
4. Visrodia K, Singh S, Krishnamoorthi R, et al. Magnitude of missed esophageal adenocarcinoma after Barrett's esophagus diagnosis: a systematic review and meta-analysis. *Gastroenterology*. 2016;150:599-607.
5. van Putten M, Johnston BT, Murray LJ, et al. 'Missed' oesophageal adenocarcinoma and high-grade dysplasia in Barrett's oesophagus patients: a large population-based study. *United European Gastroenterol J*. 2018;6:519-528.
6. De Boer E, Harlaar NJ, Taruttis A, et al. Optical innovations in surgery. *Br J Surg*. 2015;102:56-72.
7. Nagengast WB, Hartmans E, Garcia-Allende PB, et al. Near-infrared fluorescence molecular endoscopy detects dysplastic oesophageal lesions using topical and systemic tracer of vascular endothelial growth factor A. *Gut*. 2019;68:7-10.
8. Lee YJ, Krishnan G, Nishio N, et al. Intraoperative fluorescence-guided surgery in head and neck squamous cell carcinoma. *Laryngoscope*. 2012;131:529-534.
9. Warram JM, de Boer E, van Dam G, et al. Fluorescence imaging to localize head and neck squamous cell carcinoma for enhanced pathological assessment. *J Pathol Clin Res*. 2016;2:104-112.

10. Morlandt AB, Moore LS, Johnson AO, et al. Fluorescently labeled cetuximab-IRDye800 for guided surgical excision of ameloblastoma: a proof of principle study. *J Oral Maxillofac Surg*. 2020;8:1736-1747.

11. Chen J, Jiang Y, Chang TS, et al. Multiplexed endoscopic imaging of Barrett's neoplasia using targeted fluorescent heptapeptides in a phase 1 proof-of-concept study. *Gut*. 2021;70:1010-1013.

12. Linssen MD, Ter Weele EJ, Allersma DP, et al. Roadmap for the development and clinical translation of optical tracers cetuximab-800CW and trastuzumab-800CW. *J Nucl Med*. 2019;60:418-423.

13. Glatz J, Varga J, Garcia-Allende PB, Koch M, Greten FR, Ntziachristos V, Concurrent video-rate color and near-infrared fluorescence laparoscopy. *J Biomed Opt*. 2013;18:101302.

14. Koller M, Qiu SQ, Linssen MD, et al. Implementation and benchmarking of a novel analytical framework to clinically evaluate tumor-specific fluorescent tracers. *Nat Commun*. 2018;9:3739.

15. Hoy CL, Gamm UA, Sterenborg HJCM, Robinson DJ, Amelink A. Method for rapid multidiameter single-fiber reflectance and fluorescence spectroscopy through a fiber bundle. *J Biomed Opt*. 2013;18:107005.

16. Bao Q, Chatziioannou AF. Estimation of the minimum detectable activity of preclinical PET imaging systems with an analytical method. *Med Phys*. 2010;37:6070-6083.

17. Cherry SR, Sorenson JA, Phelps ME. Physics in Nuclear Medicine. Philadelphia, PA: Elsevier; 2012:244.

18. van Leeuwen–van Zaane F, Gamm UA, et al. *In vivo* quantification of the scattering properties of tissue using multi-diameter single fiber reflectance spectroscopy. *Biomed Opt*

Express. 2013;4:696-708.

19. Chen J, Yang J, Chang TS, et al. Detection of Barrett's neoplasia with near-infrared fluorescent heterodimeric peptide. *Endoscopy*. March 17, 2022 [Epub adhead of print].

20. Schölvinck DW, van der Meulen K, Bergman JJGHM, Weusten BLAM. Detection of lesions in dysplastic Barrett's esophagus by community and expert endoscopists. *Endoscopy*. 2017;49:113-120.

21. van Heijst LE, Zhao X, Gabriëls RY, Nagengast WB. Today's mistakes and tomorrow's wisdom in endoscopic imaging of Barrett's esophagus. *Visc Med*. 2022;38:182-188.

22. de Groof AJ, Struyvenberg MR, van der Putten J, et al. Deep-learning system detects neoplasia in patients with Barrett's esophagus with higher accuracy than endoscopists in a multistep training and validation study with benchmarking. *Gastroenterology*. 2020;158:915-929.

TABLES

TABLE 1: Patient characteristics. Five invisible HD-WLE dysplastic lesions were detected using FME.

	Histology				**Total**
	NDBE	LGD	HGD	EAC	(*n* = 15 patients)
Sex, male, n (%)	1 (100)	2 (100)	5 (100)	5 (71,4)	13 (86,7)
Age, mean	74.5	67.0	64.0	64.2	66
BMI, mean	28.00	27.10	27.05	27.46	27.43
Lesions identified by referring endoscopist	0	0	1	8	9 (7 patients)
Lesions identified with HD-WLE at BE expert center	0	0	3	9	12 (9 patients)
Additional NIR-FME lesions	0	2	3	0	5 (5 patients)

NDBE = non-dysplastic Barrett's esophagus, LGD = low-grade dysplasia, HGD = high-grade dysplasia, EAC = esophageal adenocarcinoma, BMI = body mass index, HD-WLE = high-definition white-light endoscopy, BE = Barrett's esophagus, NIR-FME = near-infrared fluorescence molecular endoscopy

TABLE 2: Metrics with corresponding formulas and reference values for the image quality assessment

Metric	Formula	Reference value
SNR	$20 \cdot \log 10 \frac{S}{RMSN}$	6 dB
CNR	$\frac{\lvert S - N \rvert}{RMSN}$	1

SNR = signal-to-background noise ratio, S = mean intensity signal, RMSN = root mean square noise calculated as a standard deviation from the background area, dB = decibel, CNR = contrast-to-noise ratio, N = noise calculated as a mean background signal

GRAPHICAL ABSTRACT